MULTIVARIABLE $\mathcal{H}_\infty$ CONTROLLER DESIGN AND TESTING FOR A 2.4M TELESCOPE

Paul A. Roberts [*,1,2,3] **Matthew C. Turner** [*,2]
Gustavo Medrano-Cerda [**, 3] **Ian Postlethwaite** [*,2]
Paul Rees [**, 3]

[*] *Control and Instrumentation Research Group, Department of Engineering, University of Leicester, Leicester, LE1 7RH, UK.*
[**] *Telescope Technologies Limited, Morpeth Wharf, Birkenhead, Merseyside, UK*

Abstract: This paper considers high performance motion control systems for the Azimuth axis of a 2.4m Altitude-Azimuth telescope manufactured by Telescope Technologies Limited (TTL). Tracking performance is paramount and the telescope is designed to operate with no surrounding enclosure; wind disturbances that could degrade the tracking performance are a major consideration. Previous robust control designs have used a single-input-single-output (SISO) architecture for position tracking, and this paper will assess the stability and performance of a multi-input-multi-output (MIMO) controller using simulations and test data from the real telescope. Simulations indicate that the MIMO design offers better wind disturbance rejection, and the test data show that the implementation of a MIMO control architecture is feasible.

Keywords: Robust multivariable control, H-Infinity, Telescope control

1. INTRODUCTION

Modern astronomy requires a combination of high quality optics and a precision motion control to accurately track celestial objects across the night sky. Professional observatories are usually located at high altitude sites that offer exceptionally clear sky, but these sites can also be very windy (Forbes 1982). Many existing telescope systems are housed in an enclosure designed to shield the telescope from wind disturbances, traditionally a building that supports a rotating dome with an opening slit to give a free field of view to the telescope during observations. This approach has two disadvantages. Firstly, when the telescope is tracking an object the dome must rotate with the telescope to offer a clear view of the sky through the open slit. This requires a dome control system to be implemented to synchronize the dome to the motions of the telescope. Secondly, an enclosure such as this can induce thermal turbulence in the air that refracts incoming light and degrades the quality of the images observed, an effect known as 'dome seeing' (Zago 1995). A novel way of overcoming these problems is to use an enclosure that can be completely opened up to expose the telescope to the entire sky. This approach of course re-introduces the problem of disturbances due to wind buffeting.

The telescope rotates about two axes, altitude and azimuth, both supported by hydrostatic bearings. Figure 1 shows a photo of the 2.4m telescope which is the subject of this paper. The central section of the telescope, or 'tube', is supported by two columns attached to the base box, which make up the 'yoke'. The tube rotates about the altitude axis which is perpendicular to the local vertical, and the angle of the tube with respect to horizontal is called the *elevation* (zero degrees when pointing at the horizon, ninety degrees when pointing vertically). The yoke rotates about the azimuth axis which is parallel to the local vertical. The

[1] Corresponding author: email P@ulRoberts.co.uk
[2] Supported by the UK Engineering and Physical Sciences Research Council
[3] Supported by Telescope Technologies Ltd.

dynamics of the telescope are so slow that coupling of the axes is usually negligible, especially during tracking where axis velocities are typically well below 0.5 degrees per second (P. Schipani 2001). Therefore control systems for each axis can be designed and implemented separately. Each axis is driven by two dc motors in a twin motor gear arrangement to ensure backlash-free operation. High resolution rotary encoders provide signals for the derivation of motor position and velocity. Both axis positions are derived using tape encoders to give a position resolution of less than 1.53 milliarcseconds for azimuth, less than 2.23 milliarcseconds for altitude.

Fig. 1. TTL 2.4m telescope

Previous research at TTL (Medrano-Cerda 2002) investigated and compared modern $\mathcal{H}_\infty$ methods and classical PID-type techniques in order to achieve satisfactory closed-loop tracking and disturbance rejection control of the class of telescopes described above. The key factor in both tracking performance and disturbance rejection is closed-loop bandwidth. To achieve the tracking/disturbance rejection objectives with PID methods requires a bandwidth that is too high to offer robust stability across the operational envelope of the telescope. However, using $\mathcal{H}_\infty$ methods it is possible to improve robust stability and closed-loop bandwidth and therefore the current method of choice for control system design for the TTL telescopes is $\mathcal{H}_\infty$ mixed sensitivity.

The motion control system architecture is identical for both axes and involves two feedback loops for each axis, similar to many large, ground-based telescopes (Bely 2002). An inner velocity loop provides feedback of the motor velocities while an outer position loop takes demands generated from the telescope guidance system and requires feedback of the axis position. Figure 2 shows a block diagram of the arrangement. The inner loop compensates for nonlinear friction effects at low drive velocity, and can also be tuned to correct any mismatch between the two motors. The inner loop gains are chosen in an ad-hoc manner. Currently the $\mathcal{H}_\infty$ controllers are all single-input-single-output in nature essentially constructing a control signal (fed to two motors) from a guidance system reference and the measurement of axis position. However, the motor positions are also available for measurement and it is therefore possible to construct a multi-input-multi-output (MIMO) controller for each axis. It is anticipated that such an architecture could potentially lead to improved performance and it is this architecture which will be investigated in this paper.

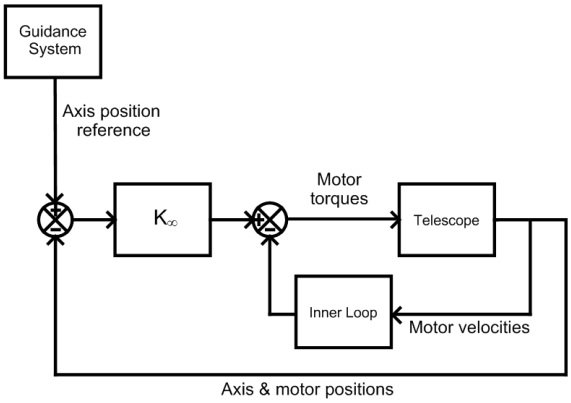

Fig. 2. Outline telescope control architecture

2. SYSTEM UNDER CONSIDERATION

2.1 Azimuth Axis model

This paper considers the multivariable control of the azimuth axis for the 2.4m telescope described above. The generic mathematical model for each axis takes the form of a second order matrix differential equation:

$$J\ddot{\Theta} = -K\Theta - D\dot{\Theta} + T \qquad (1)$$

Here J, K, and D are the inertia, stiffness and damping matrices respectively; Θ, $\dot{\Theta}$, and $\ddot{\Theta}$ represent vectors of angular position, velocity and acceleration respectively; T is a vector of external input torques (actuators and disturbances).

The azimuth axis is modelled by two inertias joined by structural stiffness and damping coefficients. Adding the dynamics of the twin drive system gives a set of second order differential equations. It is assumed that the wind disturbance torque T_d enters the dynamics at the point furthest from the drives. Figure 3 shows the azimuth model, and table 1 gives the meaning of the symbols used.

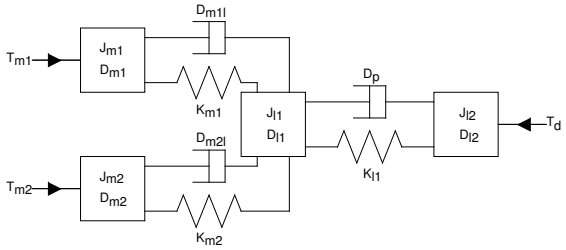

Fig. 3. Azimuth axis model

Using figure 3 the differential equations for the azimuth model are derived, which are used to calculate

Table 1. Azimuth axis model parameters

Symbol	Parameter	Units
J_{mi}	Drive inertia	$kg\,m^2$
J_{l1}	Yoke inertia	$kg\,m^2$
J_{l2}	Tube inertia	$kg\,m^2$
K_{mi}	Drive stiffness	$N\,m\,rad^{-1}$
K_{l1}	Structural stiffness	$N\,m\,rad^{-1}$
D_{mi}	Drive damping	$N\,m\,s\,rad^{-1}$
D_{mil}	Drive-axis damping	$N\,m\,s\,rad^{-1}$
D_{li}	Axis damping	$N\,m\,s\,rad^{-1}$
D_p	Structural damping	$N\,m\,s\,rad^{-1}$
T_{mi}	Motor input torque	$N\,m$
T_d	Wind disturbance torque	$N\,m$

a state space model for the axis in the standard state space realisation form

$$\dot{x} = Ax + Bu$$

$$y = Cx$$

Where

$$x = \begin{bmatrix} \Theta \\ \dot{\Theta} \end{bmatrix} \tag{2}$$

and Θ is a vector of positions of the motors and inertias shown in figure 3

$$\Theta = \begin{bmatrix} \Theta_{l1} \\ \Theta_{l2} \\ \Theta_{m1} \\ \Theta_{m2} \end{bmatrix} \tag{3}$$

The model has three inputs, the wind disturbance torque and two motor torques. Hence

$$u = \begin{bmatrix} T_d \\ T_{m1} \\ T_{m2} \end{bmatrix} \tag{4}$$

Sensors are able to measure both motor positions and the axis position, and these are the three outputs of the model. The output distribution matrix, C, is chosen so that y consists of the measured states.

$$y = \begin{bmatrix} \Theta_{l1} \\ \Theta_{m1} \\ \Theta_{m2} \end{bmatrix} \tag{5}$$

The major uncertainty in the azimuth axis model is the axis inertia due to the tube elevation angle as well as instrument payload. This can increase by 75% at elevations near horizon. Changes in this value have a significant effect on the axis resonant frequencies, which is illustrated in figure 4. This effect has stability implications for high bandwidth controllers.

The current model does not account for non-linear friction effects which are present in the real system. Stiction and other nonlinear friction effects in the drive system, particulary in the gearboxes, combined with high loop gain at low frequencies leads to limit cycles (Medrano-Cerda 2002). It is assumed that the inner velocity loop has been tuned so that these effects may be largely ignored in the $\mathcal{H}_\infty$ controller design.

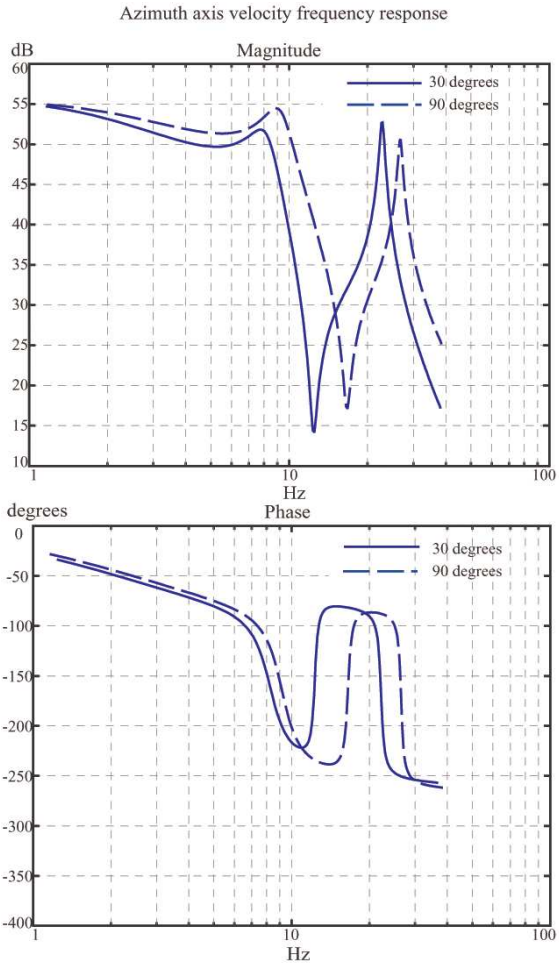

Fig. 4. Azimuth axis open loop frequency response

2.2 Wind Disturbance Model

Several models describing wind buffeting in terms of spectral densities can be used to predict the telescope performance under high velocity winds. Simulation results using the Davenport, Von Karman, Solari, Kaimal and Harris spectra show very little difference (Medrano-Cerda 2002), and the Davenport spectrum was used here to allow comparison to previous controller designs.

3. $\mathcal{H}_\infty$ CONTROLLER DESIGN

The MIMO controller was synthesised using the mixed sensitivity $\mathcal{H}_\infty$ design problem illustrated in figure 5. The controller has three inputs: axis position, motor 1 position, motor 2 position, and two outputs: motor 1 torque and motor 2 torque. The design was performed using the telescope model with 45 degrees elevation angle, i.e. with an intermediate axis inertia value, and then tested at a range of elevations. The closed loop must be stable and give acceptable performance at all elevations. Since the controller was designed to be implemented on a real system it was required that the controller was stable to reduce the possibility of runaway control signals. It was found that better disturbance rejection performance was achievable when using unstable controllers in simulation,

and although these could not be tested on the telescope this remains an area for future investigation.

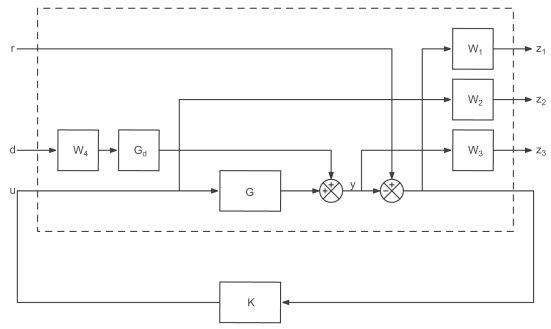

Fig. 5. $\mathcal{H}_\infty$ problem formulation

The optimization problem was thus to minimize the cost function

$$\left\| \begin{bmatrix} W_1 S & -W_1 S G_d W_4 \\ W_2 K S & -W_2 K S G_d W_4 \\ W_3 T & W_3 S G_d W_4 \end{bmatrix} \right\|_\infty \quad (6)$$

Where S and T are the sensitivity and complementary sensitivity functions respectively

$$S = (I + GK)^{-1} \quad (7)$$

$$T = GK(I + GK)^{-1} \quad (8)$$

3.1 Design weight selection

The design weights W_1, W_2, W_3 and W_4 were selected as described below.

$$W_1 = diag\{w_1, 0.0001, 0.0001\} \quad (9)$$

Good ramp tracking accuracy is required for axis position, so a second-order low-pass filter, w_1, was selected for the axis position error channel. The presence of uncertain resonances above 10Hz, as shown in section 2.1, limits the bandwidth of w_1, since the controller is required to operate at all elevations. Tracking is unimportant for the motor position outputs and so the weights on these channels were chosen with low constant values so as to have little effect on the cost function.

$$W_2 = diag\{w_2, w_2\} \quad (10)$$

A first-order high-pass filter, w_2, was used in both control signal channels, and was chosen to limit the signal magnitude at high frequencies and hence the closed loop bandwidth.

$$W_3 = diag\{w_3, 0.0001, 0.0001\} \quad (11)$$

For the weight on the axis position, w_3, a first-order high-pass filter was used. This weight was tuned to limit the closed loop bandwidth and to ensure closed loop stability for all elevations. As with the sensitivity weight, W_1, the weights on the motor positions were set at a low value constant.

$$W_4 = \frac{0.239s + 0.1095}{s^2 + 0.5976s + 0.1502} \quad (12)$$

For the weight W_4 a scaled second order low-pass filter was used, with a similar roll-off to the square root torque spectrum of the Davenport wind model.

3.2 Controller order-reduction and discretisation

For implementation the controller was truncated to 11 states via balanced truncation (Skogstad 1996) (Zhou 1990) and converted to discrete time with a sample time of 2.5ms. This was required for the controller to be compatible with the existing implementation software. A balanced realization of the controller, $K_b(s)$, was formed using the MATLAB function *sysbal*. This gives a minimal realisation of the controller with the Gramian, $\Sigma = diag(\sigma_1, \sigma_2, ..., \sigma_n)$, where each σ_i is a Hankel singular value corresponding to a particular state of $K_b(s)$, and $\sigma_i > \sigma_{i+1}$. For each state the size of the corresponding Hankel singular value gives a relative measure of the contribution of that state to the input-output behaviour of the controller. This is useful for controller order-reduction since the states that have least effect on the input-output behaviour can be identified and removed if required. Using the MATLAB function *strunc* the controller was truncated to 11 states by removing the states with the lowest values of σ, i.e. $\sigma_{12}, \sigma_{13}, ..., \sigma_n$. This reduced order controller was then discretised using Tustin's method.

4. LINEAR SIMULATION RESULTS

4.1 Frequency responses

For the MIMO system, the channel of main importance is from the axis position reference demand to the axis position output. Table 2 compares the closed loop frequency response characteristics of this channel against the SISO controller system, giving the peak values and bandwidths for the sensitivity (M_S and ω_B) and co-sensitivity functions (M_T and ω_{BT}), and the open loop gain crossover frequency (ω_c) (Skogstad 1996). These values were calculated for the system at 45 degrees elevation.

Table 2. Frequency response characteristics

Parameter	SISO	MIMO
ω_B (Hz)	1.687	2.226
M_S	1.908	1.507
ω_{BT} (Hz)	6.505	4.493
M_T	1.369	1.237
ω_c (Hz)	2.692	3.023

To compare the disturbance rejection properties of the two controllers the power spectral density of axis position due to wind buffeting torque is calculated. Figure 6 shows the error spectral density using the Davenport wind model with an average wind speed of 60 km/h.

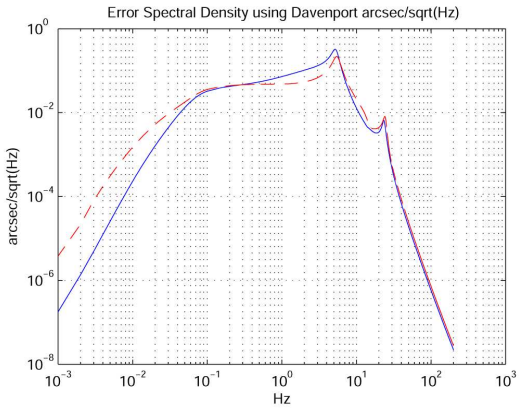

Fig. 6. Error spectral density SISO(solid) and MIMO(dashed)

The increased bandwidth of the sensitivity function, ω_B, for the MIMO controller suggests better disturbance rejection properties. This is verified by figure 6 which shows a reduction in error due to wind disturbance at the frequencies worst affected (0.1-10 Hz). The bandwidth of the co-sensitivity function, ω_{BT}, is lower for the MIMO system giving better robustness to multiplicative uncertainty, and the reduced peak values, M_S and M_T, also indicate good robustness. This is good since poor robustness could cause stability problems as the axis resonances vary with elevation. It seems that the MIMO design method enables higher 'performance bandwidths' to be combined with lower 'robustness bandwidths' more effectively than the SISO design.

4.2 Time Domain Simulations

A non-linear azimuth axis model was developed in Simulink to evaluate the system at any elevation. Simulations were carried out for the MIMO controlled system at several elevations to establish the stability and performance over the operational range of the telescope. Figure 7 shows the axis position tracking response for a step and a parabola-type reference at 0, 30, 60, and 90 degrees elevation.

The simulink model was also used to evaluate predicted RMS position errors with wind disturbance for both controllers at three elevations. The wind disturbance was modelled using the Davenport spectrum at a wind speed of approximately 40km/hr, and the simulations were run for 25 seconds.

Table 3. Simulated RMS wind errors

Elevation(deg)	SISO RMS error(")	MIMO RMS error(")
0	0.1217	0.0874
45	0.1002	0.0605
90	0.0877	0.0503

From figure 7 it can be seen that the MIMO controller offers closed loop stability at all elevations, however the effects of inertia variation are shown in the degraded quality of the step response at elevations 0 and 90 deg, i.e. those furthest from the design elevation (45 deg). The wind disturbance simulations confirm the frequency response analysis, but in addition show that the MIMO controller offers improved disturbance

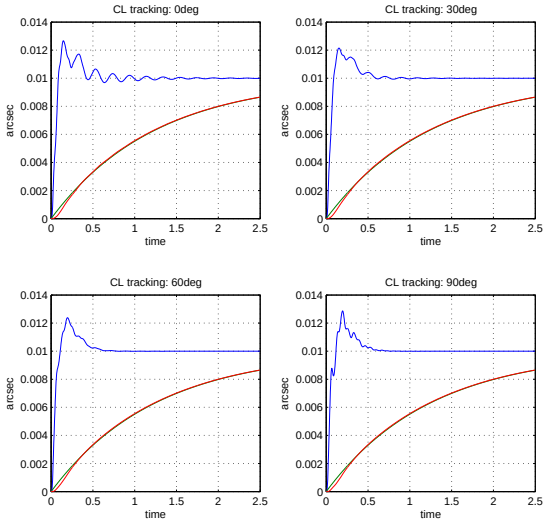

Fig. 7. Tracking and step responses for axis position across elevation envelope

rejection at all elevations. Again, the disturbance rejection performance varies with elevation, and shows a trend of improvement as the elevation angle increases, i.e. axis inertia decreases.

5. EXPERIMENTAL RESULTS

The MIMO controller was implemented on a 2.4m telescope and a series of tracking tests were performed. These tests were performed on a fully assembled telescope inside the TTL factory where the telescope was shielded from any external wind disturbances. Some of the data is presented here. Figure 8 shows the axis position response to a 15 arcseconds per second ramp reference demand at 45 degrees elevation, and also shows the response predicted by the simulink simulation. Clearly the actual system responds slower than expected, and this is most likely due to un-modelled friction effects in the drive system.

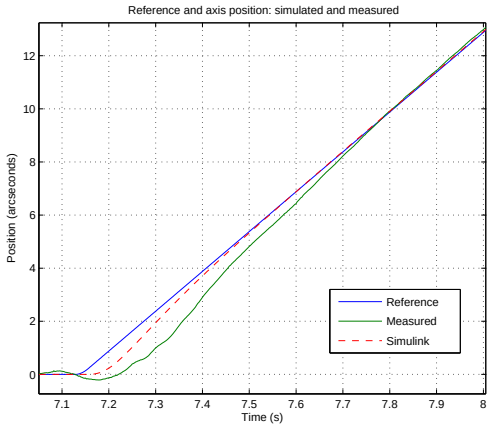

Fig. 8. Ramp tracking, 15 arcseconds/s

Tracking errors for a ramp demand of 15 arcseconds per second are shown for three elevations in Figure 9. These plots verify the simulation results that showed

the controller to be closed loop stable at all elevations. The data shows a similar trend at all elevations, an initial settling time of approximately 10 seconds, followed by good tracking with a small steady state error.

Table 4 gives values of steady state RMS axis position tracking error over a 10 second interval for a range of ramp references, at three elevations. It can be seen that the system offers comparable performance at all elevations, and the rms tracking error is around 0.5 arcseconds when tracking at 0.5 deg/s. The error value for the 60"/s ramp reference at 45° elevation seems rather anomalous, almost double the value at other elevations. This is believed to be due to a gearbox 'tight spot', i.e. a region of increased stiction at particular angular positions. This idea is supported by a detailed look at the data which reveals a limit cycle in the axis position for this test, indicating increased nonlinear friction. The test also showed the closed loop system to be stable at slewing speeds up to 2 deg/sec. This means a single controller can be used to move the axis from stationary to maximum speed without the need for a controller modification scheme as employed in some other similar scale telescopes (Mancini 1998). It is perhaps worth mentioning again that these tracking errors are without the presence of wind disturbance on the telescope, and are purely due to un-modelled dynamics such as the non-linear drive friction.

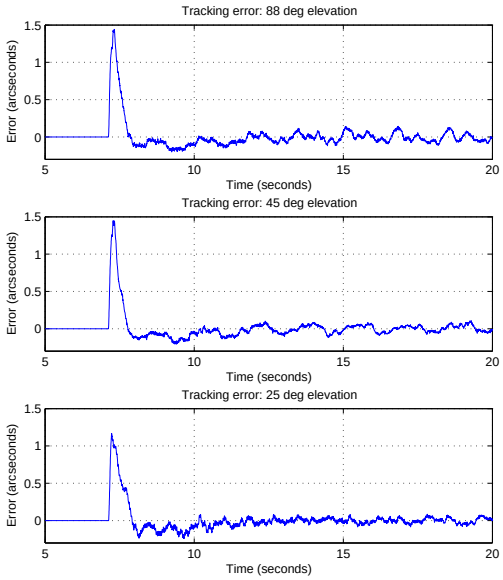

Fig. 9. Ramp tracking position error, 15 arcseconds/s

Table 4. Measured RMS axis position tracking errors for MIMO controller

Elevation	**25°**	**45°**	**88°**
Ramp("/s)	**RMS err.(")**	**RMS err.(")**	**RMS err.(")**
15	0.034	0.045	0.057
60	0.061	0.115	0.066
500	0.191	0.147	0.144
1800	0.550	0.428	0.502

6. CONCLUSIONS AND FUTURE WORK

From the simulation results the MIMO controller offers better wind disturbance rejection than the current SISO design, with RMS errors 30%-40% lower for the MIMO controller. The test data has validated the feasibility of the MIMO control architecture, and shown that the simulink model offers a reasonable simulation of the real system. Clearly, there are more detailed dynamics not captured in the model, and work into incorporating non-linear friction effects will be an area to investigate. During the controller tuning it was found that the bandwidth limitation imposed by the axis inertia variation is the main obstacle to achieving a higher performance controller. One way to overcome this would be to design multiple controllers, each operating over a smaller range of elevations but with better disturbance rejection. This would then require a scheme to transfer between controllers according to the elevation angle, and an investigation has begun into using such a scheme based on the bumpless transfer method described in (Turner 1999). It is now the intention to design a MIMO controller using $\mathcal{H}_\infty$ loop shaping techniques, which are well known for their robustness properties, and compare the results with the mixed sensitivity design approach used here. The altitude axis is modelled with an identical structure to the azimuth model, except the altitude axis does not suffer from the the same inertia variation problems. The design techniques used for the azimuth axis can therefore also be used to develop multivariable controllers for the altitude axis.

REFERENCES

Bely, P.Y. (2002). *The Design and Construction of Large Optical Telescopes*. Springer-Verlag. New York.

Forbes, F., Gabor G. (1982). Wind loading of large astronomical telescopes. *Proceedings of the SPIE Symposium of Advanced Technology Telescopes*.

Mancini, D., Cascone E. Schipani P. (1998). Telescope control system stability study using a variable structure controller. *SPIE* **3351**, 331.

Medrano-Cerda, G.A., Lett R.D. Rees P. (2002). $\mathcal{H}_\infty$ motion control system for a 2m telescope. *SPIE*.

P. Schipani, D. Mancini (2001). Vst telescope dynamic analysis and position control algorithms. *Osservatorio Astronomico di Capodimonte, Napoli, Italy* **4836**, 88–97.

Skogstad, S., Postlethwaite I. (1996). *Multivariable Feedback Control, Analysis and Design*. Wiley. New York.

Turner, M., Walker D.J. (1999). Modified bumpless transfer. *American Control Conference*.

Zago, L. (1995). The Effect Of The Local Atmospheric Envorinment On Astronomical Observations. PhD thesis. Ecole Polytechnique Fdrale de Lausanne.

Zhou, K., Doyle J.C. Glover K. (1990). *Robust and Optimal Control*. Prentice Hall. New York.